

## Stabilization of high-density atomic hydrogen in H<sub>2</sub> films at $T < 0.5$ K

J. Ahokas,<sup>1,\*</sup> O. Vainio,<sup>1</sup> J. Järvinen,<sup>1,2</sup> V. V. Khmelenko,<sup>2</sup> D. M. Lee,<sup>2</sup> and S. Vasiliev<sup>1</sup>

<sup>1</sup>*Department of Physics and Astronomy, Wihuri Physical Laboratory, University of Turku, 20014 Turku, Finland*

<sup>2</sup>*Laboratory of Atomic and Solid State Physics, Cornell University, Ithaca, New York 14850, USA*

(Received 9 April 2009; revised manuscript received 12 May 2009; published 4 June 2009)

The stabilization of high densities of atomic hydrogen ( $2 \times 10^{19}$  cm<sup>-3</sup>) embedded in solid H<sub>2</sub> films has been achieved by employing a method for producing the samples involving a direct dissociation of H<sub>2</sub> molecules by a cold plasma discharge in the sample cell at temperatures below 0.5 K. High stabilities against recombination were obtained. We observed density-dependent shifts and widths of the electron spin resonance lines resulting from the dipolar interactions between like and unlike spins. We discuss the possibilities for further increasing the H density and studying possible supersolid behavior.

DOI: 10.1103/PhysRevB.79.220505

PACS number(s): 67.80.F-, 67.80.dj, 76.30.-v

The study of matrix isolated atomic free radicals at low temperatures has had a long history. Some of the early motivation was to explore the possibility of developing high-density, low-mass systems for storing chemical energy.<sup>1</sup> The recent discovery of supersolid properties in <sup>4</sup>He (Ref. 2) has renewed interest in quantum solids. This has motivated a search for similar effects in other crystals, including hydrogen.<sup>3</sup> For pure commensurate crystals, supersolid behavior is impossible since the presence of vacancies or impurities is shown to be a required condition.<sup>4</sup> The lightest impurity atoms (H) can move through the H<sub>2</sub> crystals via quantum tunneling exchange with neighboring molecules.<sup>5</sup> The tunneling in solid H<sub>2</sub> leads to chemical exchange reactions such as  $H + H_2 \rightarrow H_2 + H$ . This process can be considered as the tunneling of a half vacancy and provides a delocalization mechanism for reaching Bose-Einstein condensation and perhaps supersolid behavior if the requisite low temperatures and high densities can be attained.

Unusual properties of atomic H in solid H<sub>2</sub> have already been demonstrated in our previous work<sup>6</sup> where we found a high stability of this system versus recombination at temperatures below 150 mK. The strong suppression of recombination was explained by the increasing role of energy level mismatch as the atoms approach each other and the temperature is lowered.<sup>7</sup> This may allow close-enough approach of the atoms without recombination, thus leading to the possibility that the wave functions overlap substantially, leading to interesting collective quantum phenomena.

So far the highest densities of H in T<sub>2</sub>-H<sub>2</sub> matrices, 270 ppm ( $\sim 7.2 \times 10^{18}$  cm<sup>-3</sup>), were obtained by dissociating molecules with 5.7 keV electrons resulting from the  $\beta$ -decay T<sub>2</sub> at  $T = 1.4$  K.<sup>8</sup> Earlier attempts to use a similar method at  $T < 1$  K failed to stabilize high densities of H due to thermal explosions of the samples.<sup>9,10</sup> In the present work we utilize a method of creating samples of H in H<sub>2</sub> with high concentrations,  $\sim 2 \times 10^{19}$  cm<sup>-3</sup>. The atoms are created by direct dissociation of H<sub>2</sub> in thin films by low energy ( $\sim 100$  eV) electrons, which are produced in the sample cell by an r.f. discharge at temperatures 100–500 mK. Our method allows us to obtain *absolutely* pure H in H<sub>2</sub> samples, containing no other impurities. We demonstrate that increasing the H density inhibits recombination and makes the system even more stable. The shapes of the electron spin resonance (ESR) lines

are determined by the dipole interaction between atoms. Our high-density samples develop a substantial magnetization in applied magnetic fields, leading to a shift in the ESR lines. We simulated the dipolar effects numerically and found a good match for the line shape and shift with the experiments.

Preparation of H<sub>2</sub> crystals with embedded H atoms starts with building a film of solid H<sub>2</sub>. The film is created by the method of slow deposition of the H<sub>2</sub> molecules resulting from recombination of H atoms in the gas phase at  $T \sim 350$  mK and in a 4.6 T magnetic field.<sup>11</sup> This method produces smooth and homogeneous films of pure H<sub>2</sub> since no other substance except H can exist in the gaseous phase and penetrate through the cold ( $< 500$  mK) sample cell (SC) filling line. To measure the thickness of the H<sub>2</sub> layer we used a quartz microbalance with one monolayer resolution. During the deposition process concentrations of atoms  $\sim 10^{18}$  cm<sup>-3</sup> could be captured in the H<sub>2</sub> film.<sup>6</sup> However, the atom populations could not be renewed once recombination took place inside the film. Therefore, in the present work we constructed a miniature dissociator utilizing low energy electrons for dissociating the H<sub>2</sub> molecules *in situ* in the film. The dissociator is a 5-mm-diameter helix made of 0.5 mm copper wire, resonating at 460 MHz and having a  $Q$  value of  $\sim 500$  [Fig. 1(a)]. R.f. power was applied to the helix in short 5–20  $\mu$ s pulses with a repetition rate of 10–500 Hz. By changing these parameters and the r.f. power we could operate the discharge in the sample cell at temperatures down to 100 mK. The average energy flux into the H<sub>2</sub> matrix during the sample preparation is  $\leq 10^{-7}$  W/cm<sup>2</sup>, low enough to keep the atoms cold and prevent them from approaching each other and recombining. In addition to the r.f. coil at the cell bottom (BC) we installed a second r.f. resonator (NMRC). It is also a helix, resonant at 910 MHz, which was originally planned to excite nuclear magnetic resonance transitions between the lower hyperfine levels of H atoms.<sup>6</sup> We also were able to run the r.f. discharge with this coil in a similar pulsed manner. The NMRC was attached to the flat mirror of the Fabry-Perot resonator, which was used to study ESR transitions in the H in H<sub>2</sub> samples and in the H gas by a cryogenic heterodyne spectrometer.<sup>12</sup>

The plasma generated by the discharge in either of the coils could be easily detected by our ESR spectrometer via strong cyclotron resonance lines of free electrons. The lines persisted for several minutes after switching off the dis-

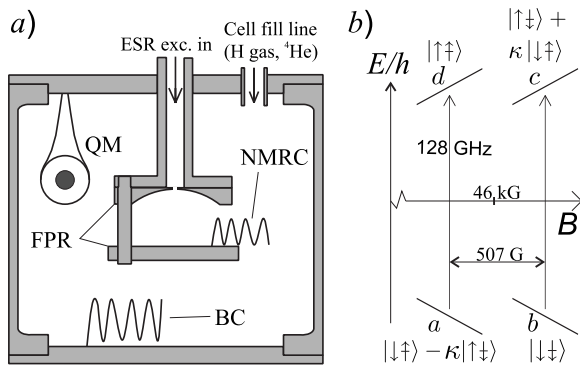


FIG. 1. (a) Experimental cell: FPR: mirrors of the Fabry-Perot resonator; BC: bottom r.f. coil; NMRC: NMR coil; and QM: quartz microbalance. (b) Hyperfine level diagram of atomic hydrogen in the strong field. Spin wave functions are labeled by projections of electron and nuclear spins and corresponding energy levels by letters a, b, c, and d.

charge, implying a long lifetime of the electrons in the SC. We estimated that the average energy of the electrons produced in the coils was  $\sim 100$  eV. Collisions of electrons with the  $H_2$  films on the walls of the SC lead to dissociation of  $H_2$  molecules in these films with a probability of  $\sim 0.2$  event/100 eV.<sup>13</sup> Some of the H atoms leave the film and desorb into the bulk gas, but the majority remains captured in the solid. The density of H atoms in the solid grows slowly as detected by the increase in the integrals of the ESR lines and reaches saturation after a couple of hours of running the discharge. The gas phase atoms could be destroyed by recombination on the SC walls when the temperature was lowered to  $\sim 100$  mK.

The density of H atoms accumulated in the  $H_2$  film could be varied by changing the deposition time and r.f. power in the discharge. With the NMRC the process was faster than with the BC, and maximal densities were a factor of 2 higher. This is because the NMRC discharge region is substantially closer to the resonator, whereas the electrons created by the BC must undergo at least one wall collision before they reach the resonator mirrors, and presumably have smaller energy and density. Optimal temperature of the SC during the discharge for obtaining highest densities was  $\sim 400$  mK. We repeated the H accumulation process for  $H_2$  films of different thicknesses. The maximum number of atoms accommodated in the film was found to be proportional to the film thickness indicating a relatively uniform concentration throughout the film.

In Fig. 2(a) we present spectra of the two ESR lines of H in  $H_2$  samples together with the lines of free H atoms in the gas phase observed in applied fields  $\sim 4.6$  T and for microwave frequencies  $\sim 128$  GHz. The low field lines (*a* line) correspond to the *a-d* transition, and the high field lines (*b* line) correspond to the *b-c* transition [see Fig. 1(b)]. The gas lines were inhomogeneously broadened, and we could reduce their width to  $\approx 30$  mG by shimming the field of our magnet. These free atom lines served as markers to find the changes in the *g* factor and hyperfine constant of the H in  $H_2$  samples. As mentioned above, the H in  $H_2$  samples were created on both mirrors of the resonator. Corresponding ESR

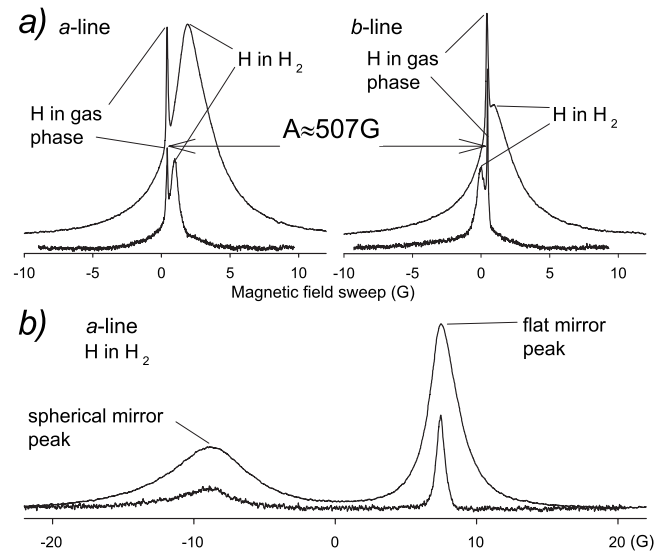


FIG. 2. (a) ESR spectra of atomic hydrogen in the gas phase and in solid  $H_2$  matrix; (b) *a* line of H in  $H_2$  sample in axial field gradient of  $\sim 20$  G/cm. For both (a) and (b) upper traces are recorded at  $n \sim 2 \times 10^{19}$   $cm^{-3}$ ; lower traces are recorded at  $n \sim 6 \times 10^{17}$   $cm^{-3}$  and multiplied by 3.5.

spectra were resolved by applying an axial gradient of magnetic field. Then, the ESR spectrum splits into two lines, as shown in Fig. 2(b), with the left peak originating from the upper spherical mirror and the right one from the flat mirror. The applied gradient has no influence on the H in  $H_2$  line-widths because of the small thickness of the films and small curvature of the spherical mirror. The substrates under the H in  $H_2$  films were different for the two mirrors: the flat mirror was covered by a 12- $\mu m$ -thick Mylar film, while the spherical mirror was bare copper following annealing and chemical etching. We found that the spherical mirror peak was inhomogeneously broadened with the width of  $\sim 6$  G, independent of the H density. The flat mirror peak was homogeneously broadened with the width proportional to H density and having a maximum value of  $\approx 2.8$  G. Integrals of both lines are proportional to the number of H atoms per unit area of the  $H_2$  film and are calibrated calorimetrically versus the density of the gas phase samples.<sup>14</sup> To obtain the bulk density  $n$  we divided the areal density by the thickness of the  $H_2$  film, measured by the quartz microbalance. This gives a maximum atomic density of  $2 \times 10^{19}$   $cm^{-3}$  with an estimated accuracy of 30%. We suggest that the inhomogeneous broadening of the spherical mirror peak is due to the substrate inhomogeneities, possibly caused by the polycrystalline structure of the pure copper surface. On the contrary, the Mylar surface is known to be very smooth and homogeneous, with weak van-der-Waals attraction to the adsorbed atoms, and therefore the flat mirror peak is better characterized.

As can be seen in Fig. 2(a), each of the H in  $H_2$  lines was shifted relative to that of the free atoms. The ESR spectrum of atomic hydrogen can be characterized by the position of the center of the spectrum and the splitting between lines. The latter is caused by the hyperfine interaction. We did not observe any dependence of this quantity on H density. By

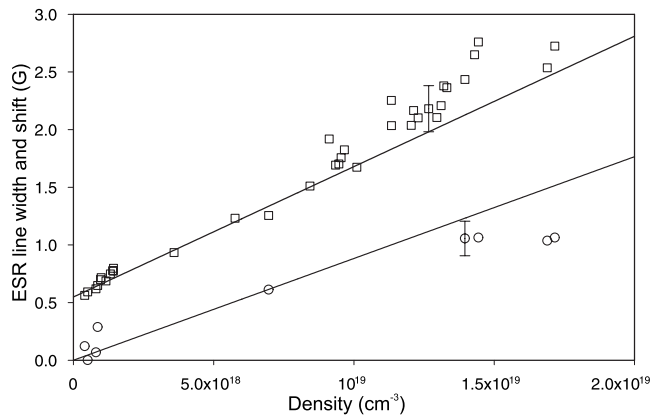


FIG. 3. □: full width at half maximum of the  $a$  ESR line originating from the flat mirror as a function of total density  $n_a+n_b$ ; ○: shift of the H in  $H_2$  ESR spectrum center from that of free H atoms as a function of density. Lines are the results of the ESR line-shape simulation as explained in the text.

measuring its deviation from that of the free atoms, we obtained the change in the hyperfine interaction for the matrix isolated atoms  $\Delta A \approx -1$  G, in qualitative agreement with the previous observations.<sup>6</sup> The negative sign of the  $\Delta A$  implies that the atoms are located in substitutional sites of the lattice. The shift of the center of the H in  $H_2$  spectrum turned out to be positive and proportional to the density  $n$  (Fig. 3). Since neither H atom or  $H_2$  molecule has orbital or quadrupolar moments, we do not find any cause for the density-dependent shift other than the magnetization of the sample. In the case of a thin film, the net dipolar field due to H atoms is directed antiparallel to the main polarizing field,<sup>14</sup> so one needs a larger field to reach the resonance. Hence the lines shift to the right. The shapes of the ESR lines were well fitted by the Lorentzian functions with the width proportional to the H density, as presented in Fig. 3. The  $\sim 0.5$  G residual linewidth as  $n \rightarrow 0$  is caused by the interactions with the nuclear spins of *orthomolecules* which are present in the  $H_2$  lattice.

The density-dependent width of the ESR spectra of H atoms indicates that the main cause of the broadening is the dipole-dipole interaction. To account for this effect on the line shapes of the spectra, we performed a numerical simulation based on the local field approximation.<sup>15</sup> We calculated the net dipolar field due to  $N=nL^2d$  spin-polarized hydrogen atoms distributed randomly inside a thin slab of thickness  $d=25$  nm and lateral dimensions  $L_x=L_y \equiv L \gg d$  oriented perpendicular to the polarizing magnetic field ( $z$  axis). The atoms were allowed to occupy any sites of the model hcp lattice equivalent to that of solid *para*- $H_2$  (lattice constant  $a=0.375$  nm) inside the slab, with the restriction that they do not approach each other by a distance closer than  $2a$ . The net dipolar field  $B_d$  due to all model atoms was calculated at the center of the slab as a function of  $z$ . The procedure was repeated  $10^4$ – $10^5$  times to calculate the probability histogram  $P(B_d, B_d + dB_d)$  for the dipolar field. Averaging the histograms over  $z$  we obtained the ESR line shape  $f(B)$ . The lines turned out to have a Lorentzian shape and are shifted to the right in the sweep field in agreement with experimental observations. Resonant interaction between

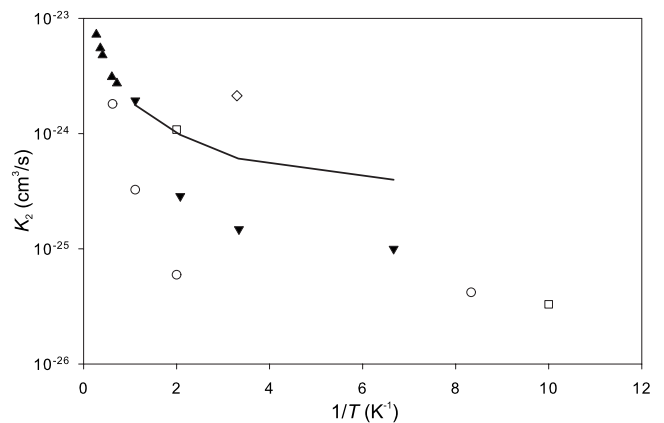


FIG. 4. Dependence of recombination rate constants of H atoms in solid  $H_2$  on reciprocal temperature. Present work: ○: high-density samples created by NMRC; □: low-density sample created by BC; and ◇: high-density samples under  $H_2$  coating. Previous experiments:  $T < 1$  K (Ref. 6): ▼;  $1.3 < T < 4.2$  K (Ref. 17): ▲. Theoretical prediction (Ref. 18) line.

identical spins (“flip-flop” transitions)<sup>16</sup> leads to an additional factor of  $3/2$  for the linewidth and shift. We observed this effect by measuring the width of the ESR line in the samples with high nuclear polarization  $n_a/n_b \sim 10$ , when most of the  $b$ -state population was transferred into the  $a$  state via the Overhauser effect.<sup>6</sup> In this case the broadening of the  $b$  line is caused mainly by unlike spins, while the  $a$  line is broadened by identical atom interactions. The width of the  $a$  line turned out to be  $\sim 1.5$  times larger than that of the  $b$  line corresponding to the  $3/2$  factor given above. For unpolarized samples  $n_a \sim n_b$  the linewidths were found to be nearly equal as expected. These correction factors for the like and unlike spin interactions were taken into account to calculate the linewidths and shifts for the samples having certain polarizations (e.g., we had  $n_a/n_b \sim 2$  for the data in Fig. 3). The results of our calculations, presented in Fig. 3 as solid lines, match the experimental data well and confirm the above-mentioned determination of absolute densities.

The possibility of easily regenerating new atoms in the  $H_2$  films allowed us to perform detailed measurements of their recombination for different temperatures and starting densities. For the highest-density samples we could not observe any decay below 1 K. However, a relatively fast decay at about 500 mK had been observed for the low-density sample  $n \sim 10^{18}$   $cm^{-3}$  created with the BC. The decays were mainly second order in density. Corresponding second-order recombination rate constants are presented in Fig. 4 along with the results of the other experimental groups and theoretical expectations.

Recombination rate constants measured in this work are substantially smaller than the rates reported in previous experiments (see Fig. 4). We explain the difference by the much higher densities in the present work. Stabilization of H atoms at high densities appears due to the energy level mismatch between the neighboring lattice sites which increases as the atoms move toward each other.<sup>7</sup> In the equilibrium case the increase in the phonon density at higher temperatures leads to a  $\sim T^9$  growth of the quantum diffusion

rate.<sup>18,19</sup> The above effects can explain our observation of the suppression of the recombination at higher densities and its enhancement during the H<sub>2</sub> coating procedure. This was manifested by a greatly enhanced recombination rate when the process of H<sub>2</sub> coating was continued by sending a high flux of H atoms through the filling line. At  $T=350$  mK the density was decreased by a factor of 2 after 12 h of such coating. A flux of high energy phonons is transferred into the film by the energetic H<sub>2</sub> molecules resulting from H atom recombination in the gas phase. This increases the probability for the atoms to hop to the next lattice site and stimulate recombination. This effect also explains why the method involving the cold discharge implemented in the present work allows us to obtain higher densities than in other methods, where much higher energy fluxes were used to generate H in H<sub>2</sub> samples. In the latter case atoms rapidly recombine during sample preparation. Further decrease in the heat released during sample preparation may be realized, e.g., by the method of cold atomic H and molecular H<sub>2</sub> beam epitaxy, when the two beams are simultaneously condensed on a cold substrate. This would produce densities exceeding  $10^{20}$  cm<sup>-3</sup>, which are expected to be stable against recombination.<sup>10</sup> To evaluate the possibility of reaching quantum degeneracy, one needs to know the effective mass  $m^* \sim \hbar^2/a^2\Delta$  of an H atom in the crystal, which is defined by the characteristic bandwidth of its tunneling motion  $\Delta$ . A typical value of  $\Delta$  is  $10^{-4}$  K for quantum diffusion of <sup>3</sup>He in <sup>4</sup>He and several degrees for vacancies.<sup>7</sup> For H in solid H<sub>2</sub>

the interval  $10^{-2} < \Delta < 1$  K has been reported.<sup>18</sup> Then, at  $n=10^{20}$  cm<sup>-3</sup> the quantum degeneracy temperature  $T^* = 2\pi\hbar^2 n^{2/3}/m^*$  ranging between 1.4–140 mK may fall into an experimentally accessible region.

In conclusion, we have demonstrated that hydrogen atoms can be created effectively in a solid H<sub>2</sub> matrix at temperatures below 1 K by direct low energy electron impact. Record high densities  $2 \times 10^{19}$  cm<sup>-3</sup> were obtained, with very high stability of the atoms. Atoms tend to avoid one another due to increasingly mismatched energy levels at near distances, which inhibits their recombination into molecules. These experiments point the way to produce H in H<sub>2</sub> samples with very high concentrations at very low temperatures. For these conditions there should be considerable wave-function overlap, which may lead to substantial quantum correlations and magnetic phenomena. With the high vacancy concentrations associated with H in H<sub>2</sub>, it may be possible to observe supersolid related effects. An advantage of the H in H<sub>2</sub> system for these investigations is that the concentration of H atoms can be controlled during experiments.

This work was supported by the Academy of Finland (Grants No. 122595 and No. 124998), the Wihuri Foundation, and the NSF (Grant No. DMR 0504683). J.A. thanks the NGS-NANO; J.J. and O.V. thank the Finnish Cultural Foundation. We thank K.-A. Suominen, R. Laiho, and S. Jaakkola for support and E. Mueller and N. Ashcroft for discussions.

\*jmiaho@utu.fi

<sup>1</sup>A. P. Bass and H. P. Broida, *Formation and Trapping of Free Radicals* (Academic Press, New York, 1960).

<sup>2</sup>E. Kim and M. H. W. Chan, *Science* **305**, 1941 (2004).

<sup>3</sup>A. C. Clark, X. Lin, and M. H. W. Chan, *Phys. Rev. Lett.* **97**, 245301 (2006).

<sup>4</sup>L. Pollet, M. Boninsegni, A. B. Kuklov, N. V. Prokof'ev, B. V. Svistunov, and M. Troyer, *Phys. Rev. Lett.* **101**, 097202 (2008).

<sup>5</sup>T. Kumada, *Phys. Rev. B* **68**, 052301 (2003).

<sup>6</sup>J. Ahokas, J. Järvinen, V. V. Khmelenko, D. M. Lee, and S. Vasiliev, *Phys. Rev. Lett.* **97**, 095301 (2006).

<sup>7</sup>Y. Kagan and A. J. Leggett, *Quantum Tunnelling in Condensed Media* (North-Holland, Amsterdam, 1992).

<sup>8</sup>G. W. Collins, J. L. Maienschein, E. R. Mapoles, R. T. Tsugawa, E. M. Fearon, P. C. Souers, J. R. Gaines, and P. A. Fedders, *Phys. Rev. B* **48**, 12620 (1993).

<sup>9</sup>R. W. H. Webeler, *J. Chem. Phys.* **64**, 2253 (1976).

<sup>10</sup>G. Rosen, *J. Chem. Phys.* **65**, 1735 (1976).

<sup>11</sup>J. Järvinen, J. Ahokas, and S. Vasilyev, *J. Low Temp. Phys.* **147**, 579 (2007).

<sup>12</sup>S. Vasilyev, J. Järvinen, E. Tjukanoff, A. Kharitonov, and S. Jaakkola, *Rev. Sci. Instrum.* **75**, 94 (2004).

<sup>13</sup>R. K. Leach, Ph.D. thesis, University of Wisconsin, 1972.

<sup>14</sup>J. Järvinen, J. Ahokas, S. Jaakkola, and S. Vasilyev, *Phys. Rev. A* **72**, 052713 (2005).

<sup>15</sup>G. W. Parker, *Am. J. Phys.* **38**, 1432 (1970).

<sup>16</sup>A. Abragam, *Principles of Nuclear Magnetism* (Oxford University Press, New York, 1961), Chap. IV, pp. 104 and 112.

<sup>17</sup>A. V. Ivliev, A. Y. Katunin, I. I. Lukashevich, V. V. Sklyarevskii, V. V. Suraev, V. V. Filippov, N. I. Filippov, and V. A. Shevtsov, *JETP Lett.* **36**, 472 (1982).

<sup>18</sup>Yu. Kagan and L. A. Maksimov, *Sov. Phys. JETP* **57**, 459 (1983).

<sup>19</sup>V. Maidaonov, A. Ganshin, V. Grigor'ev, A. Penzev, E. Rudavskii, A. Rybalko, and Y. Syrnikov, *J. Low Temp. Phys.* **126**, 133 (2002).